Distribution Agreement

In presenting this thesis as a partial fulfillment of the requirements for a degree from Emory University, I hereby grant to Emory University and its agents the non-exclusive license to archive, make accessible, and display my thesis in whole or in part in all forms of media, now or hereafter now, including display on the World Wide Web. I understand that I may select some access restrictions as part of the online submission of this thesis. I retain all ownership rights to the copyright of the thesis. I also retain the right to use in future works (such as articles or books) all or part of this thesis.

Noah Scher April 1, 2025

Adaptive response of mTOR regulation in cellular models of copper depletion

by

Noah Scher

Victor Faundez, MD, PhD
Advisor

Biology

Victor Faundez, MD, PhD

Advisor

Arri Eisen, PhD

Committee Member

Jennifer Kwong, PhD

Committee Member

2025

Adaptive response of mTOR regulation in cellular models of copper depletion

By

Noah Scher

Victor Faundez, MD, PhD

Advisor

An abstract of
a thesis submitted to the Faculty of Emory College of Arts and Sciences
of Emory University in partial fulfillment
of the requirements of the degree of
Bachelor of Science with Honors

Biology

2025

Abstract

Adaptive response of mTOR regulation in cellular models of copper depletion
By Noah Scher

Intracellular copper homeostasis is a critical cellular function required for a variety of physiological purposes including detoxification of reactive oxygen species, mitochondrial electron transport chain function, and more. To maintain a physiological balance of intracellular copper concentrations the copper importer CTR1, encoded by the *SLC31A1* gene, is localized at the plasma membrane, allowing proper influx of copper. Genetic diseases that cause brain copper depletion such as Neurodegeneration and Seizures due to Copper Transport defect (NSCT, caused by mutations in CTR1) and Menkes disease (caused by mutations in the copper transporter ATP7A) cause neuronal dysfunction and neurodegeneration. These rare genetic diseases impair activities required for the function of copper-dependent enzymes, including components of the respiratory chain and enzymes required for the synthesis of neurotransmitters and neuromodulators. We introduced a mutation which abolishes CTR1 expression, causing intracellular copper depletion similar to the phenotype of NSCT and Menkes disease. From our proteomics data, we found that the CTR1 mutant cells increased activity of the mTOR pathway, which regulates cellular functions such as gene transcription, protein synthesis, cell division and growth, and differentiation. Using the CTR1 mutant and control cell lines, we analyzed protein expression, cell viability, and bioenergetic and metabolic variability in response to pharmacological manipulations of mTOR activity. We have found that copper deficient neuroblastoma cells increase cell survival by modulating the activity of the mTOR pathway. As these pathways become clear, we will have a comprehensible understanding of the cellular response to dysfunctional copper transport and how they can be controlled to improve neurodegeneration.

Adaptive response of mTOR regulation in cellular models of copper depletion

By

Noah Scher

Victor Faundez, MD, PhD

Advisor

A thesis submitted to the Faculty of Emory College of Arts and Sciences
of Emory University in partial fulfillment
of the requirements of the degree of
Bachelor of Science with Honors

Biology

2025

Acknowledgements

I would like to thank the entire Faundez Lab for their continued support and help throughout my four years in the lab. I have grown as a scientist, individual, and member of our society in so many ways due to your impact. Special thanks to Dr. Victor Faundez for taking me in as a first-semester freshman, believing in me, and supporting me through all of the ups and downs. To Dr. Alicia Lane, I would not have been able to do this without you; this work is a combined effort of ours, and you have taught me and supported me more than you can imagine throughout my time here. To my committee members – Dr. Arri Eisen, Dr. Jennifer Kwong, and once more Dr. Victor Faundez – thank you for your support throughout this process and the time and dedication you have put into myself and this thesis. Finally, thank you to all of my friends and family who have brought me to where I am today, day in and day out.

Table of Contents

Figures & Tables

Introduction

Copper, in addition to a wide variety of metals and micronutrients, is essential to proper cell functioning, and maintaining a proper balance of it is required for a variety of physiological purposes including but not limited to detoxification of reactive oxygen species and mitochondrial electron transport chain (ETC) function as a component of cytochrome c oxidase (COX)/Complex IV (An *et al.*, 2022; Garza *et al.*, 2023). The metal is primarily obtained by dietary means and absorbed in the small intestine, where it can then be transported throughout the body (Kaler, 2022). Specifically, the blood brain barrier (BBB) is the primary site of copper entry to the nervous system. Capillary endothelial cells lining the BBB express a variety of copper transporters including ATP7A, ATP7B, and CTR1, and localize the copper transporter ATP7A to the basolateral membrane of these cells to move the copper from blood to brain (Kaler, 2022). Once in the brain, copper has a differential distribution throughout the nervous system; for example, the cerebellum is extremely rich in copper (and is of particular interest as it is one of the first regions of the brain to be severely impacted by Menkes disease, a rare childhood neurodegenerative disease related to copper imbalances) (Zlatic *et al.*, 2015), and copper is primarily associated with glutaminergic and adrenergic neurons in areas including the hippocampus, olfactory bulb, and locus coeruleus (An *et al.*, 2022; Kaler, 2022). This transport and maintenance of copper throughout the body and specifically within the nervous system is integral for development and homeostatic functioning.

To maintain a physiological balance of intracellular copper concentrations the copper transporter CTR1, encoded by the *SLC31A1* gene, is localized at the plasma membrane, allowing proper influx of copper. Genetic diseases that cause brain copper depletion such as Neurodegeneration and

Seizures due to Copper Transport defect (NSCT, caused by mutations in *SLC31A1*) (Kuznetsov *et al.*, 1996) and Menkes disease (caused by mutations in the copper transporter *ATP7A*) (Johnson *et al.*, 2013) cause neuronal dysfunction and neurodegeneration. More specifically, neurodegenerative diseases such as Menkes disease, NSCT, and others impair critical homeostatic activities that require copper-dependent enzymes, including components of the respiratory chain and other enzymes that are required for neurotransmitter and neuromodulator synthesis (Zlatic *et al.*, 2015). The mechanism(s) responsible for Menkes pathology and CTR1 deficiency remain unclear.

In addition to its role in maintaining intracellular metabolic activities and detoxifying reactive oxygen species, copper is a redox active metal which is required for oxidative phosphorylation, and as such is extremely important in homeostatic metabolic processes (Kuznetsov *et al.*, 1996). Any degree of copper toxicity or copper depletion, including dysfunctional copper transport causing copper depletion, has consequential impacts on tissues requiring high energy input and metabolic activity, such as the brain (Nagai *et al.*, 2012). Particularly, neurodevelopment is a vulnerable time for cells due to the high energy consumption and transitions in metabolism by the brain (Baik *et al.*, 2019). During fetal development, much of the energy derived by the fetal brain is created by means of glycolysis; however, there is a shift from glycolysis to mitochondrial respiration after birth (Johnson *et al.*, 2013; Donsante *et al.*, 2011; Oyarzábal *et al.*, 2021; Rajan *et al.*, 2024). This transition is widespread and is not influenced by surrounding cells or tissues, and it is observed in differentiating neurons and muscle cells in culture (Garza *et al.*, 2023; Casimir *et al.*, 2024; Iwata *et al.*, 2023; Tokuda *et al.*, 2016) and has been proven to be a key aspect in energy production for proper neurodevelopment (Casimir *et al.*, 2024; Tümer *et al.*, 2010;

Rembach *et al.*, 2013; Iwata *et al.*, 2024). Without this transition, and instead with a reliance on glycolysis for production of energy in neurons, neuronal dysfunction and damage in vitro and in vivo is observed (Jimenez-Blasco *et al.*, 2024).

The mammalian target of rapamycin (mTOR) is a possible candidate for the regulation of metabolism and protein synthesis processes in copper-deficient cells, as it is involved in a wide variety of regulatory pathways in relation to metabolic pathways. mTOR is a protein kinase that controls a variety of intracellular mechanisms and signaling pathways, including but not limited to cellular metabolism, survival, proliferation, and nutrient homeostasis. It can form one of two complexes (mTORC1 and mTORC2), and it catalyzes the phosphorylation of several proteins such as AKT, protein kinase C (PKC), and ribosomal protein kinase S6 (S6K) thereby activating them and promoting protein synthesis (Panwar *et al.*, 2023).

Here, we postulate that increased intracellular mTOR signaling is an adaptive mechanism in response to copper depletion. By understanding how copper-depleted cells, which exhibit the phenotypes that are observed in Menkes disease and similar copper-related neurodegenerative diseases like NSCT, respond to stressors such as small molecule drugs, copper chelators, and inhibitors of the mTOR pathway, we can better understand how intracellular signaling, cellular viability, and metabolism are impacted by a balance between copper depletion and resiliency mechanisms that increase cellular fitness to copper depletion (Khan *et al.*, 2017). The balance between adaptive and non-adaptive processes is likely to impact multiple genetic defects causing neurodevelopmental and neurodegenerative phenotypes. Furthermore, as we understand more about the mechanisms by which both glycolytic and mitochondrial bioenergetic pathways

contribute to the neuronal phenotypes observed in Menkes disease, and the mechanisms of their regulation, we will have a greater understanding of the pathology of Menkes and other neurodegenerative conditions such as Parkinson's disease, which we have established is genetically linked to Menkes disease (Comstra *et al.*, 2017).

To phenocopy this copper depletion, we generated two models of copper depletion: *SLC31A1*-null cells that cannot import copper via the CTR1 copper transporter on the plasma membrane and *ATP7A*-LA cells that fix the ATP7A copper transporter to the plasma membrane, causing endogenous copper extrusion. ATP7A sequesters cytosolic copper into the Golgi and responds to intracellular copper by moving to the cell membrane and extruding excess copper from the cell (Liu *et al.*, 2013). ATP7A is expressed throughout the body (Kaler, 2011), and loss-of-function ATP7A mutations deplete the brain of copper because the organism is unable to absorb dietary copper and release it into the bloodstream (Tümer *et al.*, 2010; Kaler, 2011). **Fig. 1** summarizes these two distinct models.

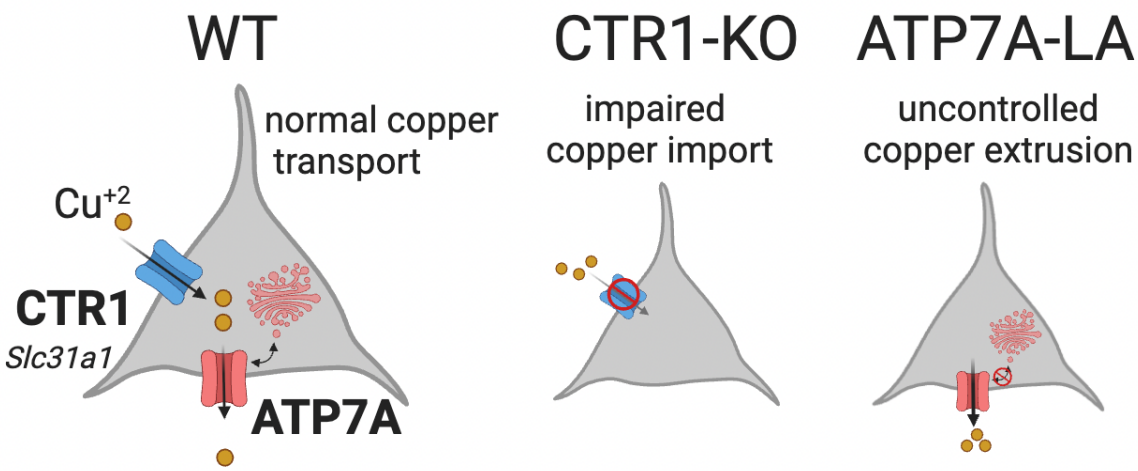

Fig 1. Cellular models of copper depletion. Under normal conditions, copper homeostasis is maintained in part by import of copper to the cell by CTR1 and extrusion of excess copper from the cell by ATP7A. To phenocopy neuronal copper depletion observed in Menkes disease, we generated isogenic SH-SY5Y CTR1-KO and ATP7A-LA cells that will exhibit disrupted copper uptake or uncontrolled copper extrusion, respectively.

Based on our pharmacogenomics, cellular viability, protein synthesis, and bioenergetic studies, we have determined that activation of the mTOR pathway and upregulation of protein synthesis is an adaptive mechanism by which cells fundamentally depleted of copper maintain their function.

Materials & Methods

Cell lines, gene editing, and culture conditions

Human neuroblastoma SH-SY5Y cells were grown and maintained in DMEM media supplemented with 10% fetal bovine serum (FBS) at 37° C in 10% CO_2 unless otherwise noted. SH-SY5Y cells with a loss of *SLC31A1* were generated via genome editing using guide RNA and CRISPR-Cas9 preassembled complexes by Synthego with a KO efficiency of 97%. The guide RNAs used were UUGGUGAUCAAUACAGCUGG, which targeted transcript ENST00000374212.5 exon 3. Wild-type and mutant cells were cloned by limited dilution and mutagenesis was confirmed by Sanger sequencing with the primer: 5'GGTGGGGGCCTAGTAGAATA. All controls represent either a single wild-type clone or a combination of two wild-type clones. All experiments used two separate mutant clones of cells (KO3 and KO20) to exclude clonal or off-target effects unless otherwise indicated. Similarly, SH-SY5Y cells with a loss of *ATP7A* were also generated via genome editing using guide RNA and CRISPR-Cas9 with a model fit of 97%. The guide target was ACCTGACAAGCACTCACTCC and a PAM sequence of TGG. All controls represent either a single wild-type clone or a combination of two wild-type clones. All experiments used two separate mutant clones of cells (LA58 and LA63) to exclude clonal or off-target effects unless otherwise indicated.

Antibodies

The antibodies used in these experiments for Western blots are listed in **Table 1** at their indicated concentrations.

Antibody	Dilution	Catalogue Number	RRID
Actin B	1:5000	Sigma-Aldrich A5441	AB_476744
ATP7A	1:500	NeuroMab 75-142	AB_10672736
CCS	1:500	ProteinTech 22802-1-AP	AB_2879172
COX17	1:500	ProteinTech 11464-1-AP	AB_2085109
CTR1 (SLC31A1)	1:2000	ProteinTech 67221-1-IG	AB_2919440
DBH	1:500	Millipore AB1536	AB_2089474
DEPTOR	1:1000	Cell Signaling 11816	AB_2750575
HSP90	1:1000	BD Biosciences 610418	AB_397798
mTOR	1:1000	Cell Signaling 2983	AB_2105622
mTOR pSer2448	1:1000	Cell Signaling 5536	AB_10691552
OXPHOS mix	1:250	Abcam ab110412	AB_2847807
PERK (EIF2AK3)	1:1000	Cell Signaling 5683	AB_10841299
RAPTOR	1:1000	Cell Signaling 2280	AB_561245
RICTOR	1:1000	Cell Signaling 2114	AB_2179963
S6K pThr389	1:1000	Cell Signaling 9234	AB_2269803
mouse HRP	1:5000	A10668	AB_2534058
rabbit HRP	1:5000	G21234	AB_2536530

Table 1. Antibodies

Drugs

The drugs used in these experiments, including those used for viability and Synergy assays, immunofluorescence and blotting, and Seahorse metabolic oximetry assays, are listed in **Table 2** at their indicated concentrations.

Drug	Source/Catalogue Number	Storage/Stock	Concentration range
Elesclomol	VWR, 101758-608	1 mM, DMSO, -20°C	1 nM - 1024 nM
Copper chloride	Sigma, 203149	120 mM, water, -20°C	25 µM - 600 µM
BCS	Sigma, B1125	400 mM, DMSO, -20°C	0.1 mM - 1.6 mM
Oligomycin	Sigma, 75351	10 mM, DMSO, -20°C	1.0 µM
FCCP	Sigma, C2920	10 mM, DMSO, -20°C	0.25 µM
Rotenone	Sigma, R8875	10 mM, DMSO, -20°C	0.5 µM

Antimycin A	Sigma, A8674	10 mM, DMSO, -20°C	0.5 µM
Emetine	Sigma, E2375	100 mM, DMSO, -20°C	2 nM - 2500 nM
Puromycin	Sigma, P7255	10 mg/mL, DMSO, -20°C	1 mg/mL
Insulin	Sigma, 91077C	1 mM, water, 4°C	1.6 nM - 1000 nM
Torin-2	VWR, 103542-338	1 mM, DMSO, -20°C	1 nM - 250 nM
Rapamycin	VWR, 101762-276	50 mM, DMSO, -20°C	0.8 µM - 66 µM

Table 2. Drugs

Western blotting

Cells were grown up to required confluency for these experiments and subsequently washed and lysed using lysis buffer containing 150 mM NaCl, 10 mM HEPES, 1 mM ethylene glycol-bis(β-aminoethylether)-N,N,N,N-tetraacetic acid (EGTA), and 0.1 mM MgCl2, pH 7.4 (Buffer A), with 0.5% Triton X-100 (Sigma, T9284) and Complete anti-protease (Roche, 11245200). Cells were then scraped from the plates and placed in Eppendorf tubes on ice for 20 min, followed by centrifugation at 16,100 × g for 10 min. The clarified supernatant was recovered from the tubes, and the Bradford Assay (Bio-Rad, 5000006) was then used to determine protein concentration. All lysates were flash frozen on dry ice and stored at −80°C. Samples were prepared accordingly to load onto 4-20% Criterion gels (Bio-Rad, 5671094) for SDS-PAGE in running buffer (25 mM TRIS, 130 mM glycine, and 0.1% SDS) and transferred using the semidry transfer method to polyvinylidene difluoride (PVDF) membranes (Millipore, IPFL00010) with transfer buffer (48 mM TRIS, 39 mM glycine, 0.037% SDS, 20% methanol). The membranes were incubated in TBS (1.36 M NaCl, 26.8 mM KCl, 247 mM TRIS) containing 5% nonfat milk and 0.05% Triton X-100 (TBST; blocking solution) for 30 min at room temperature, followed by washing and incubating the

membrane in primary antibody in a solution containing PBS with 3% BSA and 0.2% sodium azide overnight. The next day, the membranes were washed in TBST and incubated in secondary antibodies against mouse or rabbit (see **Table 1**) diluted 1:5000 in the blocking agent for at least 30 minutes at room temperature. Following incubation, the membranes were washed 3 times in TBST and then probed with Western Lighting Plus ECL reagent (PerkinElmer, NEL105001EA) and exposed to GE Healthcare Hyperfilm ECL (28906839).

Cell survival and Synergy analysis

For viability assays utilizing a single drug, cells were counted using a Bio-Rad cell counter (Bio-Rad, TC20, 1450102) plated into 96-well plates at concentrations of 5,000-10,000 cells per well. The cells were then treated with the chosen drug (see **Table 2** and figure legends for exact concentrations used) and allowed to incubate for 48-72 hours. Fresh DMEM media with 10% Alamar blue (Resazurin, R&D Systems #AR002) was added to each well and incubated for 2 hours, followed by absorbance measurements using a microplate reader (BioTek, Synergy HT; excitation at 530–570 nm and emission maximum at 580–590 nm) with Gen5 software 3.11 as a proxy for cell count. For single-drug assays investigating the effects of elesclomol, experiments were conducted in DMEM media containing either glucose or galactose. Percent survival was calculated by subtracting the background value of a well without cells (and therefore only Alamar blue) and normalizing to the untreated condition for each genotype. All experiments contained treatment conditions in duplicate or triplicate.

For Synergy assays, cells were counted, treated, and measured in the fashion described above with combinations of various drugs and conditions (see Table 2 and figure legends for exact conditions used). Percent survival was similarly calculated by normalizing to the untreated condition for each genotype. For the experiments with serum addition and removal (those with fetal bovine serum, FBS) absorbance values were normalized to the 10% serum condition which is the serum concentration in normal DMEM growth media. All experiments contained treatment conditions in duplicate or triplicate. SynergyFinder online software was used to calculate synergy ZIP scores and quantitatively analyze relationships.

Seahorse metabolic oximetry

Extracellular flux analysis of the Mito Stress Test was performed using the Seahorse XFe96 Analyzer (Seahorse Bioscience) following the recommendations of the manufacturer. SH-SY5Y (CTR1 control and KO) cells were seeded at concentrations of 30,000 cells per well in Seahorse XF96 V3-PS Microplates (Agilent Technologies, 101085-004), following trypsinization and counting using the Bio-Rad TC20 automated Cell Counter the day before the assay. XFe96 extracellular flux assay kit probes (Agilent Technologies, 102416-100) were incubated with the manufacturer calibration solution at 37°C without CO2 injection overnight before the assay. On the day of the assay (one day following cell seeding), the cells were washed twice in Seahorse XF base media (Agilent Technologies, 102353-100), and washed a third time in Seahorse XF base media with the addition of the chosen conditions (seen in **Table 3**). In these varying media conditions, cells were incubated at 37°C without CO2 injection for 1 h prior to the stress test.

During this incubation period, flux plate probes were loaded and calibrated. Following calibration, the flux plate containing calibrant solution was exchanged for the Seahorse cell culture plate and equilibrated. Seahorse injection ports were filled with 10-fold concentrated solution of oligomycin A, FCCP, and rotenone mixed with antimycin A (refer to **Table 2** for final testing concentration of Seahorse drugs and catalogue numbers). All Seahorse drugs were dissolved in DMSO and diluted in Seahorse Mito Stress Test Media for the protocol. The flux analyzer protocol included an hour-long period of basal read cycles following injection of oligomycin A, FCCP, and rotenone mixed with antimycin A. Each read cycle included a 3 minute mix cycle followed by a 3 minute read cycle where oxygen consumption rate (OCR) and extracellular acidification rate (ECAR) were determined over time. Following the assay, cells were washed twice with PBS (Corning 21-040-CV) supplemented with 1 mM $MgCl_2$ and 100 µM $CaCl_2$, and then lysed with Buffer A mixed with Complete Protease Inhibitor Cocktail (Sigma Aldrich). Protein concentration was measured using the Pierce bicinchoninic acid (BCA) Protein Assay Kit (Thermo Fisher Scientific, 23227) following the manufacturer protocol. The BCA assay absorbance was read by a BioTek Synergy HT microplate using Gen6 software. All experimental conditions were done in duplicate, where individual data points represent the average values. Nonmitochondrial respiration was determined as the lowest OCR following injection of rotenone plus antimycin A. Basal respiration was calculated from the OCR just before oligomycin injection minus the nonmitochondrial respiration. Nonmitochondrial respiration was determined as the lowest OCR following injection of rotenone plus antimycin A. ATP-dependent respiration was calculated as the difference in OCR just before oligomycin injection to the minimum OCR

following oligomycin injection but before FCCP injection. Maximal respiration was calculated as the maximum OCR of the readings following FCCP injection minus nonmitochondrial respiration.

Condition	**Supplemented With**
Base Medium	Seahorse XF Base Medium, pH adjusted with sodium hydroxide (NaOH)
Glutamine (0.1-2 mM)	Seahorse XF Base Medium (pH adjusted w/ NaOH), 200 mM glutamine
Glutamine (2 mM) and pyruvate (1 mM)	Seahorse XF Base Medium (pH adjusted w/ NaOH), 200 mM glutamine, 100 mM pyruvate
Glucose	Seahorse XF Base Medium (pH adjusted w/ NaOH), 200 mM glutamine, 100 mM pyruvate, 2.5 M/45% glucose
Galactose	Seahorse XF Base Medium (pH adjusted w/ NaOH), 200 mM glutamine, 100 mM pyruvate, 500 mM galactose

Table 3. Seahorse media conditions

Results

CTR1 and ATP7A-LA mutant cell lines are fundamentally depleted of copper

Our mutant cell lines phenocopying Menkes disease and NSCT (i.e., copper depleted phenotypes) were generated via CRISPR genome editing (**Fig. 1; Fig. 2, Panels A and B**). Using inductively coupled plasma mass spectrometry (ICP-MS) (Wilschefski and Baxter, 2019; Lane *et al.*, 2022), we confirmed that both of our mutant cell lines were copper depleted (**Fig. 2, Panel C**), although to different extents. Even more, we further characterized the CTR1-KO cells as they proved to show an increased resistance to copper and decreased levels of the copper-dependent Golgi enzyme dopamine-β-hydroxylase (DBH, **Fig. 2, Panel D**). Copper is also highly regulated and involved in the assembly and function of Complex IV of the electron transport chain (Zeng *et al.*, 2007), and the protein abundance of mitochondrial Complex IV in CTR1 KO cells was up to 55% less than that of the wild type (**Fig. 2, Panel E**). Other subunits and complexes of the transport chain remained unchanged (**Fig. 2, Panel E**). With this data, we are confident that our gene editing was successful in our mutant cell lines and confidently moved forward with further characterization and experiments.

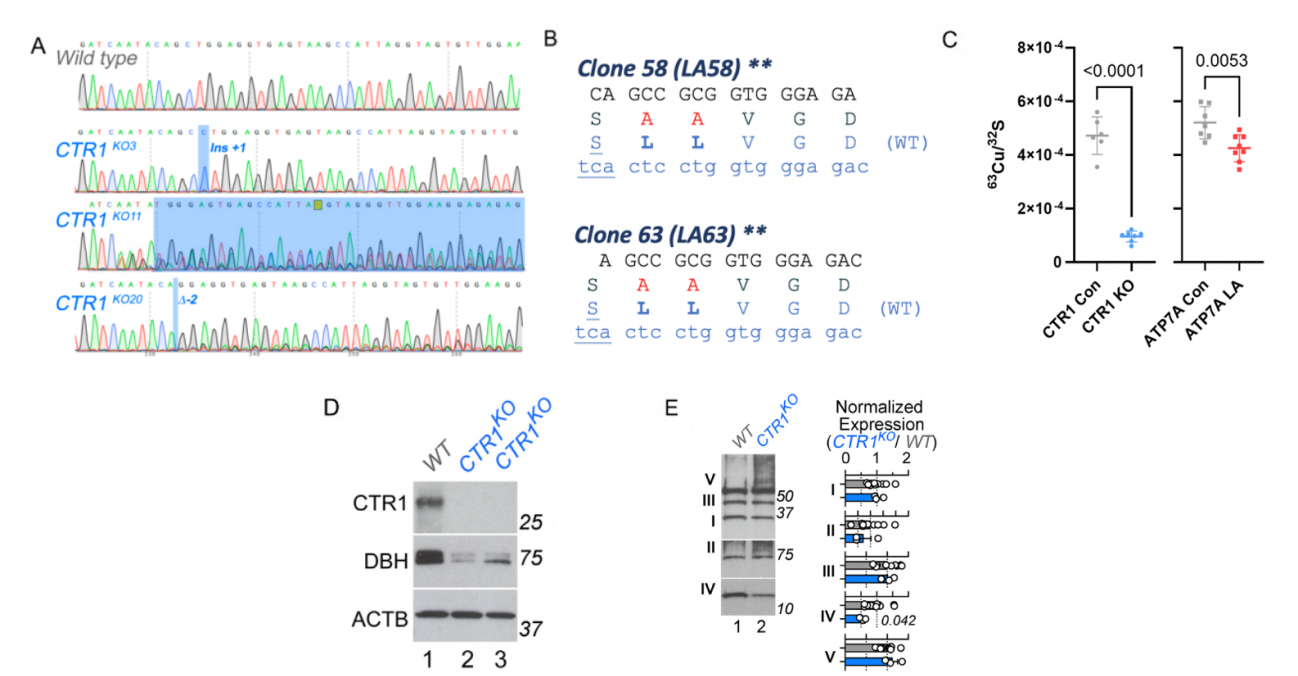

Fig. 2. Generation and characterization of CTR1 knockout and ATP7A mutant neuroblastoma cells. A. DNA sequence chromatograms of one wild type and three SLC31A1 CRISPR-edited SH-SY5Y clonal lines. Blue boxes mark the mutated sequence. B. Mutations of the ATP7A second LL motif. Variants in the Wild-Type DNA change the protein structure from two leucine's to two alanine's. C. ICP-MS of CTR1 KO and mutant ATP7A cells and their controls, presented as copper content treated with vehicle, normalized to 32S. D. Immunoblot of cellular extracts from wild-type (lane 1) and two independent SLC31A1 Δ/Δ mutant (CTR1 KO, lanes 2–3) SH-SY5Y cell clones probed for CTR1 and DBH with beta-actin as a loading control. E. Immunoblot with OxPhos antibody mix in mitochondrial fractions from wild-type and CTR1 KO cells. Complex II was used as a loading control as it does not form respiratory supercomplexes (Iverson et al., 2023). (Each dot is an independent biological replicate. Italicized numbers represent p values analyzed by two-sided permutation t test.).

Cell viability in response to elesclomol and bathocuproine disulphonate (BCS)

Using either the copper ionophore elesclomol which delivers copper directly to the mitochondria (Kirshner *et al.*, 2008; Wu *et al.*, 2011; Blackman *et al.*, 2012; Soma *et al.*, 2018; Garza *et al.*, 2022) or the copper(II) chelator bathocuproine disulphonate (BCS), we measured cell viability in response to increasing concentrations in our wild-type and ATP7A-LA mutant cell lines. In response to increasing elesclomol concentrations up to 512 nM, we found no significant difference in the viability of our control and LA mutants (**Fig. 3,** left panel). We further probed this by switching our DMEM media to DMEM media containing galactose (rather than glucose).

This switch forced the WT and LA mutants to rely strictly on oxidative phosphorylation rather than glycolysis for energy production (Marroquin *et al.*, 2007). Similarly, we found no significant difference in the viability of WT and ATP7A-LA mutants (**Fig. 3,** compare left and middle panels). Therefore, the similarities between our WT and mutant responses are accounted for; however, there is increased cell death in response to lower doses of elesclomol in galactose media as compared to glucose media. Without glucose to stimulate glycolysis as a means of energy production, both our WT and ATP7A-LA mutants were not as viable in response to low doses of elesclomol indicating that glycolysis is imperative for cellular function at both homeostatic and reduced copper levels. We then tested the effect of increasing concentrations of BCS on cell viability and found a significant difference between WT and ATP7A-LA response. WT cells remained viable across increasing concentrations of BCS; however, the ATP7A-LA mutants had reduced survival in concentration of BCS greater than or equal to 800 µM (**Fig. 3,** right panel).

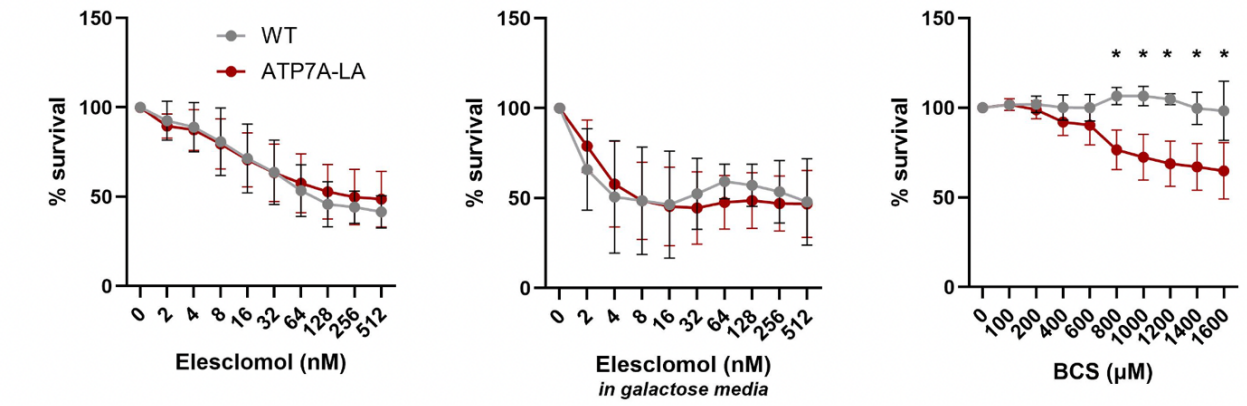

Fig. 3. Cell survival analysis of ATP7A-LA mutants with increasing concentrations of elesclomol or BCS. Average ± SD for all, representing percent survival relative to untreated cells in each condition. As for the elesclomol conditions, n = 8 for both controls and mutants in standard DMEM media while n = 3 for both controls and mutants in DMEM media supplemented with galactose. For BCS conditions, n = 4 for controls and n = 10 for mutants. Asterisks represent a significant difference, with a p-value < 0.005.

Increased activation of mTOR-Raptor-S6K signaling and protein synthesis in CTR1 proteome and phosphoproteome

The mammalian target of rapamycin (mTOR) is a candidate for the regulation of metabolism and protein synthesis processes in copper-deficient cells, as it is involved in a wide variety of regulatory pathways in relation to metabolic pathways (Lane *et al.*, 2025; see **Fig. 7**). We aimed to identify pathways and signal transduction mechanisms that are altered in scenarios of copper deficiency similar to Menkes disease and NSCT. From our quantitative tandem mass tagging mass spectrometry (TMT-MS) of the whole cell and phosphorylated proteomes, in the CTR1 proteome and phosphoproteome we identified 210 proteins and 224 phosphopeptides that were expressed in levels significantly different than those found in the wild type ($p < 0.01$, fold change ≥ 1.5, **Fig. 4, Panels A and B**). Of these, 153 proteins and 138 phosphopeptides were present at higher concentrations, while 57 proteins and 86 phosphopeptides were present at lower concentrations in the CTR1 KO cells. Furthermore, we found that the mTOR signaling pathway is upregulated in the CTR1 knockout proteome and phosphoproteome by investigating the NCATS Bioplanet discovery resource with the ENRICHR tool and multiple databases with the Metascape tool (ENRICHR q=1.4E-3 and Metascape q=5.01E-10, **Fig. 4, Panel C**) (Huang *et al.*, 2019). From further studying and analyzing the CTR1 knockout proteome and phosphoproteome, we found significantly pronounced changes in many proteins directly related to mTOR signaling, including increased phosphorylation of mTOR and RPS6. Activation of the mTOR pathway was confirmed by Nanostring nCounter transcriptomics and has led us to believe that mutations in CTR1 modify the proteome and signaling pathways of copper-deficient cells, converging on mTOR signaling pathways regulating protein synthesis. Therefore,

we conclude there is a connection between mTOR signaling in response to a deficiency in copper-dependent metabolism.

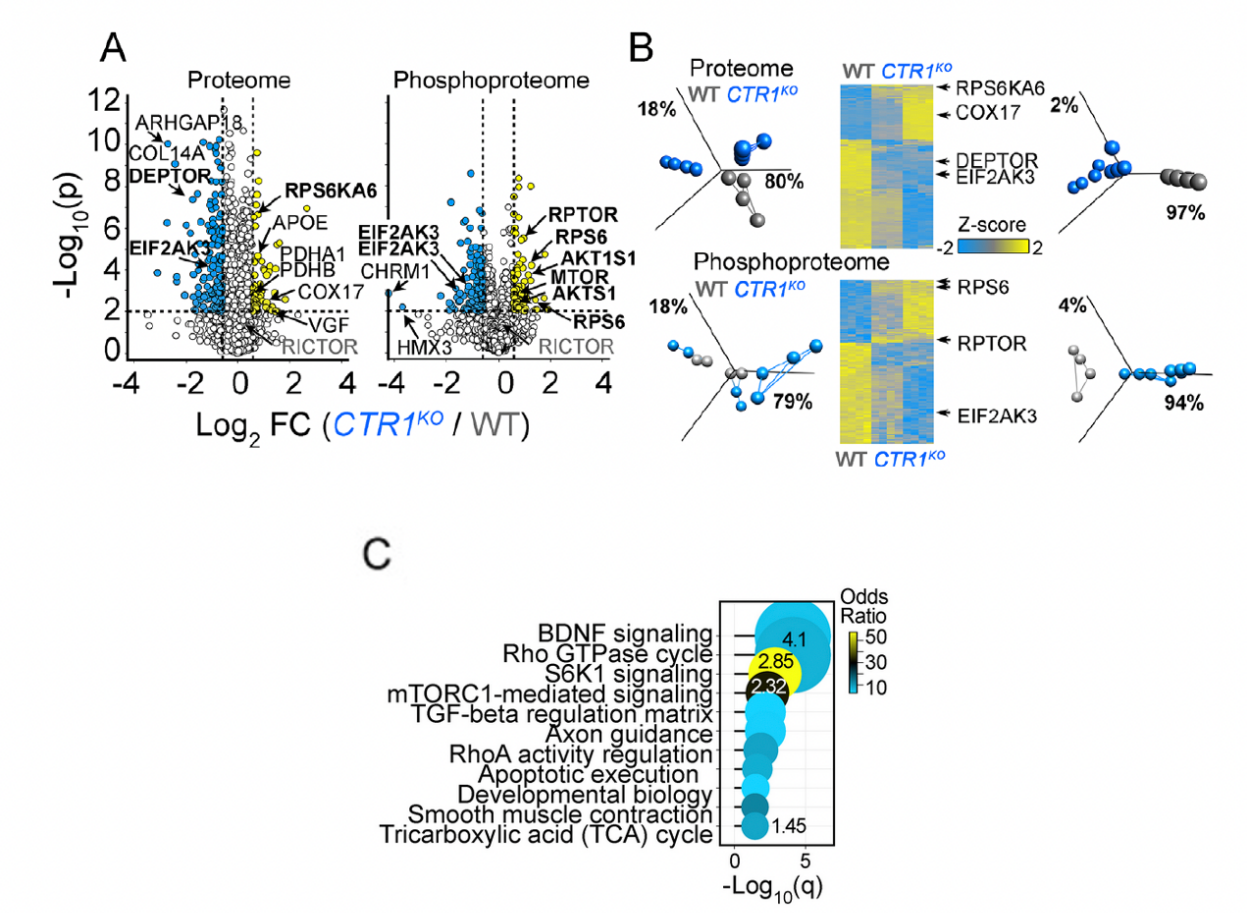

Fig. 4. Increased mTOR-Raptor-S6K signaling in the CTR1 KO proteome and phosphoproteome. A. Volcano plots of the CTR1 KO cell proteome and phosphoproteome (TMT1), where yellow dots represent proteins or phosphoproteins whose expression is increased in KO cells and blue dots represent decreased expression in DO cells. n = 4 for wild-type cells and n = 3 for KO cells in two independent clones (KO3 and KO11). B. Principle component analysis (PCA) of the whole proteome and phosphoproteome from wild type (gray) and two CTR1 KO clonal lines (blue symbols). Hierarchical clustering of all proteome and phosphoproteome hits where differential expression is significant with $q < 0.05$ and a fold change of 1.5 (*t* test followed by Benjamini-Hochberg FDR correction). C. Gene ontology analysis of differentially expressed proteins or phosphopeptides in CTR1 mutant proteome and phosphoproteome. Bioplanet and KEGG databases were queried with the ENRICHR engine. Fisher exact test followed by Benjamini-Hochberg correction.

mTOR signaling activation and upregulation is necessary for CTR1 KO cell survival

Utilizing various combinations of specific drugs to manipulate the mTOR signaling pathway, we used Synergy assays and the associated Zero-Interaction Potency (ZIP) model to analyze synergistic and/or antagonistic relationships between drugs and their effects on cell viability (Ianevski *et al.*, 2022). A ZIP score greater than 10 indicates that the relationship between the drugs is likely to be synergistic (the additive effects of the drugs are greater than the individual effects of the drugs alone), while a ZIP score less than -10 indicates that the relationship between the drugs is likely to be antagonistic (the additive effects of the drugs are less than the individual effects of the drugs alone) (Yadav *et al.*, 2015). A ZIP score between -10 and 10 assumes that there is no interaction between the drugs, and their combined effects are similar to the individual effect of each drug (Yadav *et al.*, 2015). To analyze these relationships, we pharmacologically manipulated mTOR and copper levels and quantified WT and CTR1 knockout viability and response.

First, we analyzed the response to fetal bovine serum (FBS) with various drugs that manipulate (either activating or inhibiting) the mTOR pathway. FBS is a growth supplement that activates mTOR signaling pathway activity, and depletion of serum therefore reduces mTOR signaling (Liu and Sabatini, 2020). Rapamycin is an mTORC1 pathway inhibitor, which inhibits mTOR signaling completely, while Torin-2 is an ATP-competitive mTOR inhibitor that blocks the binding of ATP and subsequent substrate-level phosphorylation (Ballou and Lin, 2008; Zheng and Jiang, 2015). Based on our hypothesis that activation of mTOR signaling is necessary for survival in copper depleted cells, a synergistic relationship between FBS and mTOR inhibitors would indicate that activity of the mTOR pathway is detrimental to the cells and would cause increased cell death,

while an antagonistic relationship between them would indicate that upregulation of the mTOR pathway is necessary for cell survival in models of copper depletion phenocopying copper-dependent neurodegenerative diseases. In fact, the latter proved to be true and there was an antagonistic relationship between FBS and drugs that inhibit mTOR signaling, which is more pronounced in the CTR1 KO cell lines as compared to the WT (ZIP score between -22.1 to -27.7 for WT and -30.9 to -34.6 for CTR1 KO, **Fig. 5, Panels A-D**). This data indicates that CTR1 KO cells, which as we established are fundamentally depleted of copper, are reliant on mTOR signaling for survival as inhibiting mTOR is even more harmful when paired with the pro-survival effects provided by FBS.

Furthermore, we found that our copper-deficient CTR1 KO cells are dependent on mTOR activity for their survival specifically in a copper-dependent manner. When investigating the combined effects of mTOR inhibition with either elesclomol or bathocuproine disulphonate (BCS), a copper ionophore and chelator, respectively, we found that delivering copper directly to the cells via elesclomol rendered the CTR1 KO cells more resistant to increasing concentrations of Torin-2, an mTOR inhibitor (ZIP score between -35.6 to -38.3 for WT and -33.8 to -37.9 for CTR1 KO, **Fig. 5, Panels E-F**). Conversely, mTOR inhibitors in combination with BCS negated ZIP score differences between the genotypes (**Fig. 5, Panel C**). Altogether, the findings from our Synergy assays support our hypothesis that the activation of the mTOR signaling pathway is an adaptive response to copper depletion in our CTR1 KO mutant cells.

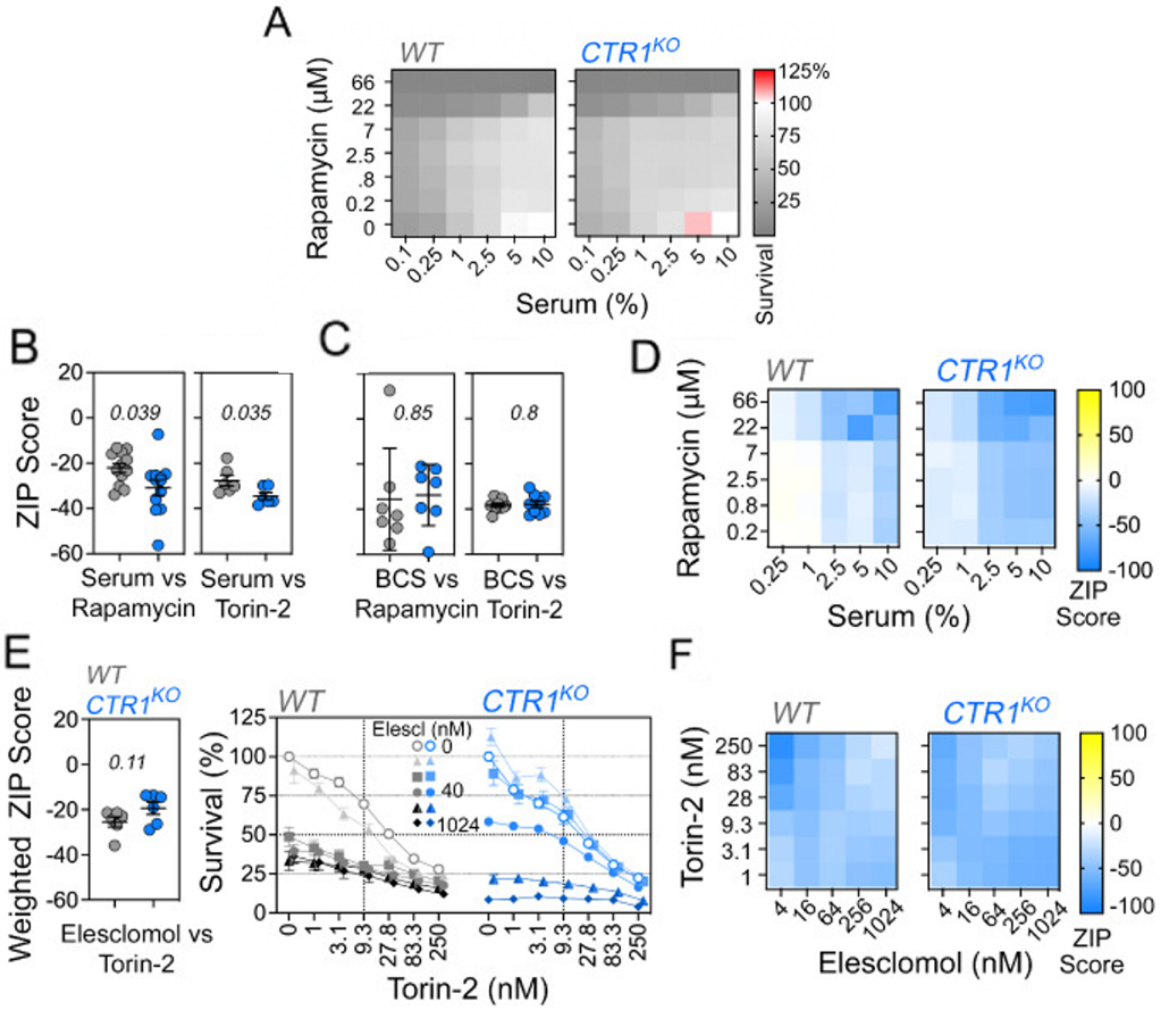

Fig. 5. CTR1 KO increases susceptibility to mTOR inhibition. A-F. Synergy analysis of cell survival of CTR1 mutants treated with increasing concentrations of combinations of the compounds serum, rapamycin, Torin-2, BCS, and elesclomol. A. Cell survival map for cells treated with serum and rapamycin, with the corresponding interaction synergy map calculated using the Zero Interaction Potency (ZIP) score for cell survival (D). B-C,D-F. Scores below -10 indicate an antagonistic interaction between the compounds. Maps were generated with at least six independent experiments per pair that generated percent cell survival maps and average ZIP score for drug interactions in B or weighted ZIP score in D. Average ± SEM, two-sided permutation t-test. D-F. Synergy analysis of CTR1 mutants with increasing concentrations of Torin-2 and elesclomol, with different colors and symbols indicating increasing concentrations of elesclomol (E) with average weighted ZIP score (D, two-sided permutation t-test) and elesclomol ZIP interaction synergy map (F).

Increased activity of the mTOR pathway

Since our findings from our proteomics and phosphoproteome data indicated an upregulation of mTOR signaling, we analyzed steady-state levels of mTOR and related proteins in our WT and CTR1 KO cells. From Western Blot, we found that CTR1 KO cells exhibit decreased CTR1 (abolished expression, as expected), DEPTOR, and EIF2AK3 (PERK), as well as increased expression levels of the copper chaperone COX17 (**Fig. 6, Panel A**). However, there were no changes in ATP7A or CCS expression, two proteins that are frequently altered in models of copper depletion (**Fig. 6, Panel A**) (Bertinato *et al.*, 2003; Kim *et al.*, 2010). To test our hypothesis of increased mTOR signaling in response to copper depletion, we measured the expression of mTOR and S6K (a downstream indicator of mTOR activity) as well as their phosphorylation statuses. As serum (Fetal Bovine Serum, FBS) promotes mTOR-S6K signaling pathway activity (or reduces it via serum depletion) (Liu and Sabatini, 2020), we used serum addition and depletion paradigms, respectively. As sensors of mTOR and S6K activity, we focused on the S2448 residue for mTOR and the T389 residue for S6K for phosphorylation sites, as mTOR S2448 is within the catalytic domain and is a target of S6K itself and S6K T389 is phosphorylated in an mTOR-dependent manner (Navé *et al.*, 1999; Reynolds *et al.*, 2002; Cheng *et al.*, 2004; Chiang and Abraham, 2005). Overall, we observed a greater increase in the phosphorylation of mTOR and S6K in the CTR1 KO mutant cells as compared to the WT cells as serum was added back to supplement the cells. Additionally, after being depleted of serum overnight, there was greater phosphorylation in the CTR1 KO cells as compared to WT (**Fig. 6, Panel B**, lanes 1 and 5), and as serum was progressively added back to the cells after initial depletion, mTOR and S6K phosphorylation continued to increase to a larger extent in the CTR1 KO cells than in the WT (**Fig. 6, Panel B**, lanes 2-4 and 6-8). Similarly, in cases

of serum depletion alone, CTR1 KO cells exhibited increased levels of mTOR and S6K phosphorylation and activity than WT at baseline and following the depletion (**Fig. 6, Panel C**). This data indicates that CTR1 KO cells have increased steady-state levels of expression of mTOR and S6K (and therefore increased mTOR-related signaling) and rely on its signaling as a protective mechanism in response to copper depletion.

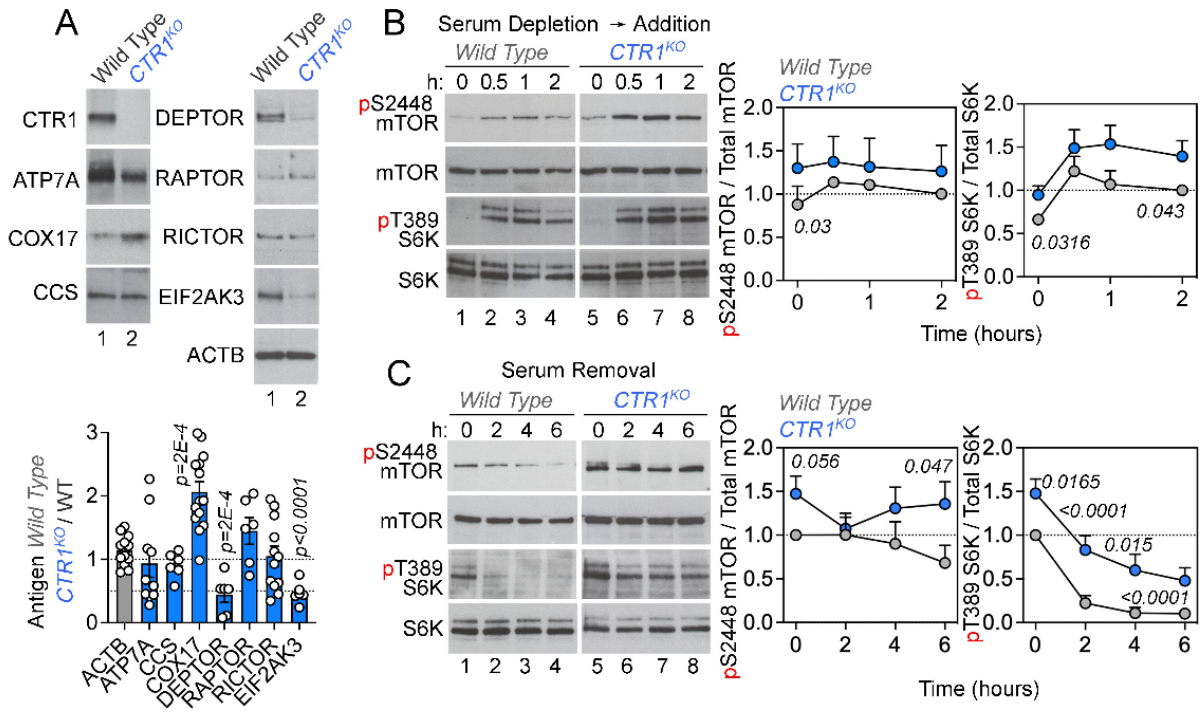

Fig. 6. Increased activity of the mTOR-S6K pathway in CTR1 KO cells. A. Immunoblots of whole-cell extracts from WT and CTR1 mutant SH-SY5Y cells with actin as a loading control, quantified by normalizing expression to WT cells. **B, C.** Immunoblots with antibodies detecting phosphorylated or total mTOR or S6K as loading controls after overnight serum depletion and addition (B) or at time 0 followed by depletion (C), normalized to control at time 0 (C) or time at 2 hours (B). (Two-Way ANOVA followed by Benjamini, Krieger, and Yekutiel corrections).

Adaptive metabolic processes of CTR1 mutants in response to copper depletion and increased mTOR signaling

From our preliminary findings of baseline metabolic processes in our copper-deficient CTR1 mutant cells, we found decreased basal and ATP-dependent respiration as compared to the wild-

type (0.53x and 0.54x comparable wild-type levels; **Fig. 7, Panels A and B**, compare columns 1 and 2). We performed Seahorse metabolic oximetry using the Mito Stress Test to observe these metabolic responses to copper deficiency. The differences noted above were specific to CTR1 KO-related copper deficiency as treatment with the copper chelator bathocuproine disulphonate (BCS) magnified the differences (**Fig. 7, Panel B**, compare columns 1 and 8) while having no effect on the wild-type (**Fig. 7, Panel B**, compare columns 1 and 7). Using elesclomol at low, nontoxic concentrations rather than BCS to deliver copper to the cells, the respiration defects observed in the CTR1 mutants were rescued and there was increased media acidification of the knockouts, indicating increased glycolysis (**Fig. 7, Panel B**). To further characterize these glycolytic parameters of the CTR1 KO, we used the Glycolysis Stress Test and found that the mutants exhibit increased extracellular acidification, glycolysis (2.03x wild-type levels), and glycolytic capacity (1.18x wild-type levels), while exhibiting decreased glycolytic reserve (0.20x wild-type levels) (**Fig. 7, Panel C**). These findings have indicated that impaired respiratory and metabolic function in the CTR1 KO cells have caused a metabolic shift that favors glycolysis over oxidative phosphorylation.

Given these differences, we continued to investigate the metabolic phenotypes of our wild-type and mutants in varying conditions. Since mTOR activation could lead to an increase in the efficiency of protein synthesis and cell cycle progression by increased amino acid uptake (Ma and Blenis, 2009), we began to investigate the metabolic response to different sources of energy and amino acids. From Seahorse metabolic flux assays, we found that wild-type and CTR1 knockout mutant cells respond similarly to conditions of varying energy sources, including Seahorse media containing glucose, galactose, glutamine, or void of any supplements (**Fig. 7, Panels D and E**). There were slight differences in certain elements of the mitochondrial stress test, including

pronouncedly lower basal respiration rates in the CTR1 knockouts as compared to the wild-types, and slightly lower proton leak levels in the knockout (**Fig. 7, Panel D**). On the other hand, the spare respiratory capacity was higher in the knockouts than the controls (**Fig. 7, Panel D**). Without much of a difference in the respiration within each genotype throughout the varying conditions, we decided to push both genotypes further and investigated whether differing concentrations of glutamine would have an effect on respiration, as glutamine is one of multiple amino acids used as a sensor for mTOR signaling and regulation (Bodineau *et al.*, 2022). Similarly, there was no stark difference in the respiration between genotypes in specific varying conditions (**Fig. 7, Panel E**). Both genotypes had higher rates of respiration when supplied with glucose as a primary energy source (with the CTR1 mutants having lower baseline respiration overall) and depriving the cells of glutamine down to concentrations of 0.1 mM slightly rescued the oxygen consumption rate of both genotypes from base medium, but not by a significant amount. This data continues to confirm that the CTR1 mutant cell line, which is deprived of copper, adaptively responds to copper deficiency in manners that go beyond protein synthesis and signaling pathway regulation, but in a metabolic manner as well. The CTR1 knockout cells have dramatically different respiratory rates and metabolic processes than their control counterparts, however when pushed to near deprivation of glutamine (an amino acid essential for mTOR signaling), respiration remains stable indicating there is some other protective mechanism at play. Further study is required to elucidate these novel findings.

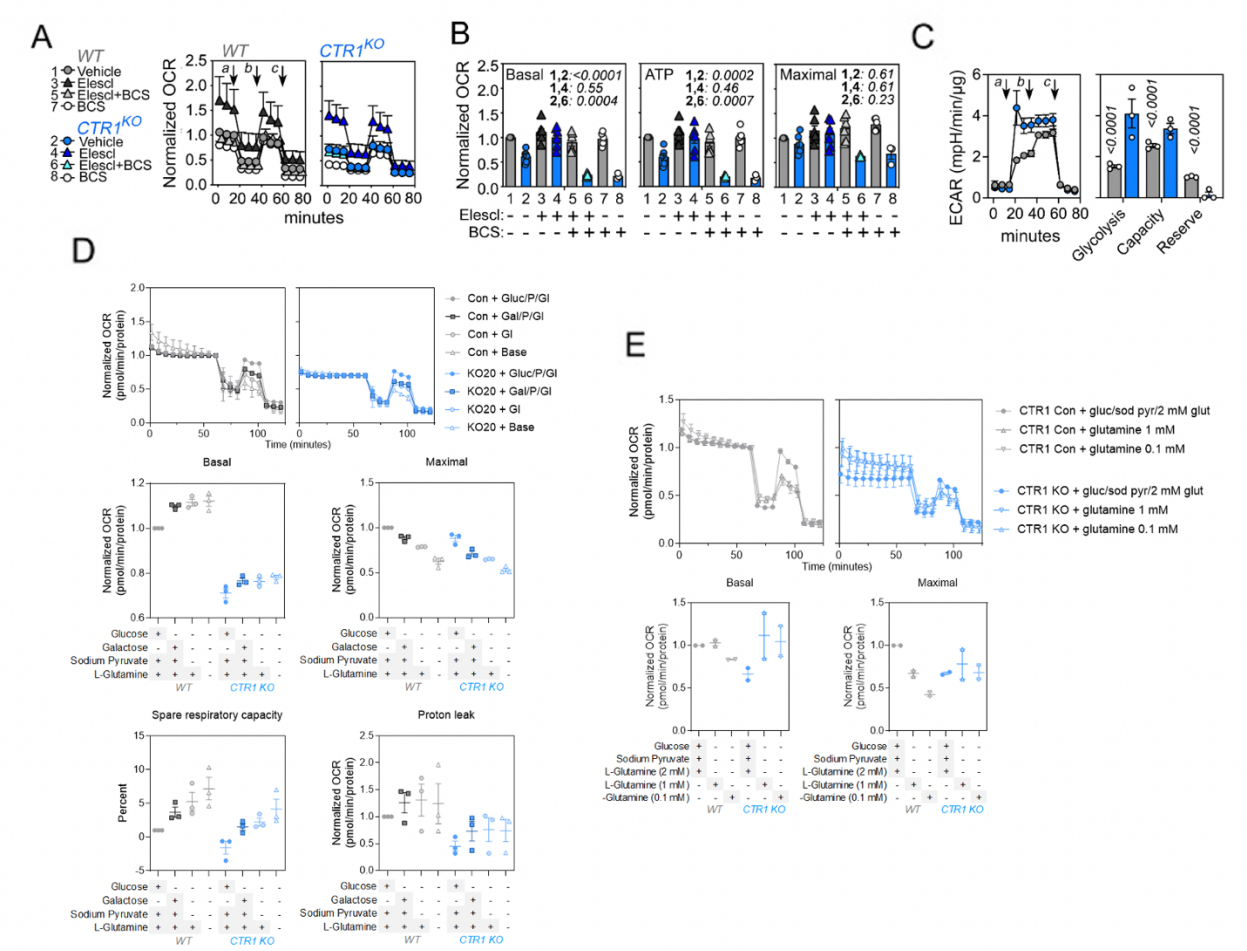

Fig. 7. Similar metabolic activity of CTR1 controls and mutants in varying energy conditions and amino acid composition. A-E. Seahorse metabolic flux assays and stress tests in wild type and CTR1 KO cells. Arrows indicate the sequential addition of oligomycin (a), FCCP (b), and rotenone-antimycin A (c) in the Mito Stress Test. CTR1 clone KO20 was used. All data presented as average ± SEM. **A.** Cells treated with vehicle, 1 nM elesclomol, or 200 µM BCS for 72 hours (BCS n = 3, other treatments n = 6-7). Basal cellular respiration was measured for 90 minutes after additions using Seahorse. **A-C.** Data is presented normalized to basal respiration of wild-type cells in the absence of drug, analyzed by a one-way ANOVA followed by Benjamini, Krieger, and Yekutieli multiple comparisons correction (italics show q values). **C.** Arrows indicate the sequential addition of glucose (a), oligomycin (b), and 2-DG (c) in the Glycolysis Stress Test (n = 3). **D-E.** Basal cellular respiration was measured for 60 minutes prior to the addition of any drugs. Cells were washed and incubated in chosen conditions prior to assay. Presented normalized to time = 10 minutes.

Discussion

Here, we show that an upregulation of mTOR signaling and adaptations to homeostatic protein synthesis are adaptive mechanisms by which cells respond to copper deficiency. This has been confirmed in our cellular models, and is also proven in our animal models, of copper depletion (data not included; Lane *et al.*, 2025).

We established the cellular models of copper depletion by utilizing CRISPR-Cas9 genome editing to modify *CTR1* and *ATP7A* copper transporters in SH-SY5Y neuroblastoma cells. We confirmed that these cells (both the wild-type and mutant genotypes) were deprived of copper, which phenocopies the severe neurodegenerative diseases and conditions of interest, specifically NSCT and Menkes disease. With decreased intracellular copper concentrations, molecular changes occurred affecting copper-dependent enzymes, complexes, and signaling pathways involved in a variety of critical cellular functions. However, there are certain drugs that can revert metabolic phenotypes caused by copper depletion such as elesclomol (**Figure 7**), which has been proven to rescue the neurodegenerative symptoms and phenotypes in animal models of copper depletion and copper-related neurodegenerations (Guthrie *et al.*, 2020; Yuan *et al.*, 2022). Elesclomol sequentially binds copper outside of the cell, facilitating its uptake as an elesclomol-Cu(II) complex followed by subsequent generation of reactive oxygen species (ROS). Thus copper, with an oxidation state of +2, is brought directly to the mitochondria of the cells and induces oxidative stress (Garza *et al.*, 2022) and upon dissociation the drug can transport back to the extracellular milieu to begin the process again. Further studies are necessary to understand the full effects of the use of drugs such as elesclomol as therapeutics for copper-related neurodegenerative diseases.

With respect to our ATP7A-LA mutants and drugs modifying copper content, both our control and mutant cell lines had similar viability in response to increasing concentrations of elesclomol and showed no difference when forced to rely on oxidative phosphorylation in a galactose-mediated environment. We are continuing to explore the mechanisms by which cells respond to ATP7A mutations and resulting copper depletion and aim to find the functionality of these intracellular adaptations the mutant cells make to respond similarly to our controls. However, since there is no significant difference in the mutant cells' ability to respond to this direct transport of copper to the mitochondria, we hypothesized about the impact of direct loss of copper using the copper chelator bathocuproine disulphonate and its direct effect on the dileucine mutation.

Looking more in depth into our research using BCS and copper chelation, we now have proven that BCS provides greater cell death in our LA mutant lines compared to our control cell line (**Figure 3**). This is also a clear difference from the use of the copper chelator PSP2 which chelates Cu(I), the intracellular form of copper, instead of Cu(II), the copper that BCS directly binds (**Supplemental Figure 1**) (Heuberger *et al.*, 2019). The functionality and mechanisms of action behind the cell responses of our controls and mutants remain unclear, as well as if there is a fundamental difference in the response to extracellular chelation of copper versus intracellular copper chelation. However, we hypothesize that the effects of PSP2 chelating intracellular copper suggest that the distribution of copper in intracellular compartments, in particular mitochondria, may be similar between LA and control cells. Such model would account for the similarity of effect when cells are treated with elesclomol. We continue to explore these questions, as well as how BCS and a clear deficiency of intracellular copper is affecting the survival of our cells at higher

concentrations of the drugs. We hypothesize that BCS is forcing the cells to rely on glycolysis for ATP production instead of mitochondrial respiration, and that copper depletion through BCS is predictive of an increase in glycolysis. Importantly, our data has led us to the finding that the mTOR pathway may be involved in regulating these changes in metabolism.

Globally, copper depletion increased mTOR signaling within the cell, which was seen to be an extremely enriched term from our NCATS and Bioplanet query (**Figure 4**). Increased phosphorylation of the protein RPS6, indicating a greater amount of activity, has validated this finding as it appropriately suggests that there is an increase in the level and activity of the mTOR-S6K signaling pathway (**Figure 6**). Furthermore, there is less expression of the protein DEPTOR, which is an inhibitor of mTOR signaling (Peterson *et al.*, 2009); one stop that is homeostatically placed on mTOR pathway activation has been released allowing its upregulation (**Figure 6**). It is evident that our copper-deficient cells (specifically the CTR1 KO genotype) are dependent on mTOR signaling and downstream adaptations of protein synthesis as some sort of protective mechanism against the lethal effects of depleted copper. This is seen by our findings of increased levels and phosphorylation of mTOR and S6K in the CTR1 mutant cells by Western blotting (**Figure 6**) at both baseline conditions and over conditions of serum depletion and addition paradigms.

Copper-related neurodegenerative diseases, as well as more broad and translational neurodegenerative diseases such as Alzheimer's disease and Parkinson's disease, have associated bioenergetic and mitochondrial dysfunction (Oyarzábal *et al.*, 2021; Johnson *et al.*, 2013; Khan *et al.*, 2017). This dysfunction has been proven to be related to mTOR and PERK signaling in our CTR1 KO cells (Lane *et al.*, 2025), which gives us a framework to understand the

upregulation of mTOR activity in our copper-depleted models that phenocopy NSCT and Menkes disease. Our pharmacogenomics, Synergy, and cell viability studies have allowed us to understand not only that copper-deficient cells rely on upregulation of mTOR signaling as a means of survival but that they regulate mTOR signaling in a copper-dependent manner. The question now lies in why these cells would upregulate mTOR signaling, a pathway in which signaling is dependent on its environment, in scenarios of copper deficiency rather than saturation.

It is possible that this increase in mTOR signaling and adaptations of protein synthesis in our cellular models of copper depletion could be a mechanism by which these cells remedy the imbalance of proteostasis and metabolism due to the copper deficiency itself (Lane *et al.*, 2025). Autophagic flux is the rate at which intracellular damaged materials are processed and broken down by the lysosomes, and it has been reported that there is impaired autophagic flux in hyperglycolytic neurons (Jimenez-Blasco *et al.*, 2024). Furthermore, copper is required for proper activity of Unc-51-like autophagy activating kinase 1 (ULK1) activity and for autophagy in general (Tsang *et al.*, 2020), therefore copper deficiency may inhibit autophagy and limit the availability of amino acids that are derived from recycled materials post lysosomal degradation. In this scenario, increased mTOR activation could be a method by which copper depleted cells increase the efficiency of protein synthesis and progression through the cell cycle via increased amino acid uptake. In our CTR1 KO cells and WT cells treated with BCS, we have found that there is increased mRNA for the amino acid transporters SLC7A5 and SLC3A2 (**Supplemental Figure 2**), indicating that there is an increased demand for amino acids for *de novo* protein synthesis. mTOR activation, as well as the upregulation of specific elements and chaperones of the electron transport chain

(ETC) such as COX17 (a copper-specific chaperone for complex IV), may be a mechanism by which these cells can utilize nutrients and maintain their viability in an otherwise nutrient void environment (in respect to copper and potentially a limited pool of amino acids).

These findings are what prompted our metabolic studies in various conditions as if these cells are reliant on increased mTOR signaling, downstream adaptations to protein synthesis, and possibly increased amino acid transport in relation to copper depletion, we would expect their bioenergetics and metabolism to vary between genotypes. As seen (**Figure 7**), there is a fundamental difference in the respiration and metabolism of our control and copper deficient CTR1 knockouts with the mutant respiration being around 50% less than that of the controls (Lane *et al.*, 2025). However, our more recent experiments have not yet uncovered genotype-condition specific differences. In conditions of almost no glutamine (0.1 mM), which would be expected to push these cells to their extremes in terms of what is available in their environment, responses across genotype-conditions were consistent indicating some other protective mechanism these cells are using for respiration in extreme environments. It remains possible that the maximal respiration of the CTR1 knockout is higher when pushed to the extremely limited glutamine conditions (0.1 mM as compared to 1 mM) as compared to the control, however conclusions such as this cannot be made at this time. This speculation requires additional studies investigating the uptake and use of specific amino acids, resulting respiration and metabolic changes, and dependency on mTOR activation and inhibition.

Our cellular models of copper depletion that phenocopy Menkes disease and NSCT, including our ATP7A-LA mutants and our CTR1-KO mutants, provide strong evidence that genetic defects

impairing intracellular copper homeostasis resulting in extreme copper deficiency cause changes in both cellular signaling pathways and critical cellular functions such as protein synthesis (**Figure 8**). The manner by which the mTOR signaling pathway is regulated in these environments is copper-dependent and environmentally adaptive (**Figure 8**). Overall, we propose that these genetic and bioenergetic changes are adaptive responses to pathological copper depletion, shedding new light on rare neurodegenerative mechanisms that remain unclear.

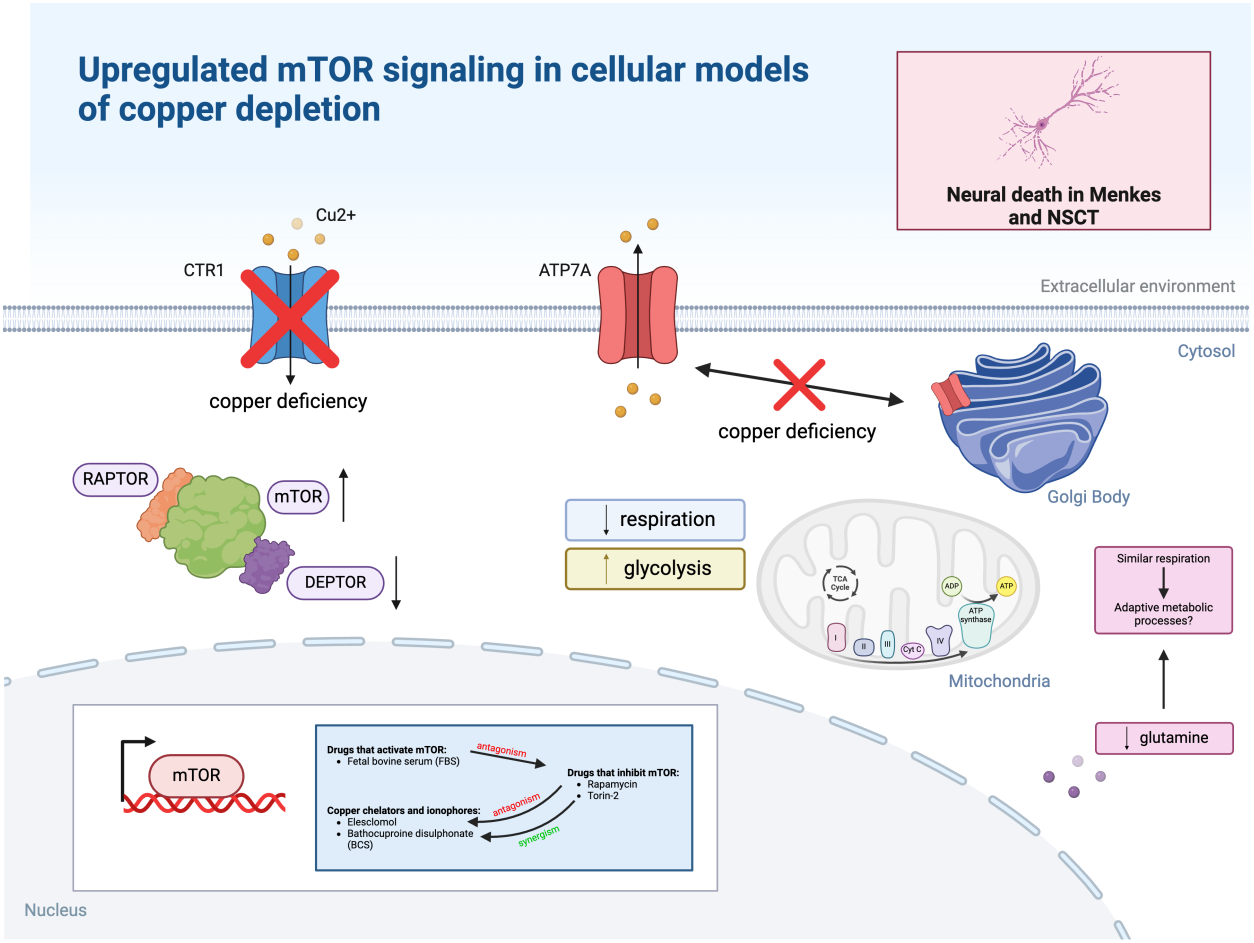

Fig. 8. Upregulated mTOR signaling as an adaptive and protective mechanism in cellular models of copper depletion. Via viability and Synergy assays, immunoblots, and Seahorse metabolic oximetry we have found that increased mTOR signaling is an adaptive mechanism by which CTR1 mutant cells respond to copper deficiency.

References

A, O., M. U, B. Lf, and G.C. A, 2021 Energy metabolism in childhood neurodevelopmental disorders. *EBioMedicine* 69:103474.

An, Y., S. Li, X. Huang, X. Chen, H. Shan *et al.*, 2022 The Role of Copper Homeostasis in Brain Disease. *Int J Mol Sci* 23 (22).

Ash, D., V. Sudhahar, S.W. Youn, M.N. Okur, A. Das *et al.*, 2021 The P-type ATPase transporter ATP7A promotes angiogenesis by limiting autophagic degradation of VEGFR2. *Nat Commun* 12 (1):3091.

Baik, S.H., S. Kang, W. Lee, H. Choi, S. Chung *et al.*, 2019 A Breakdown in Metabolic Reprogramming Causes Microglia Dysfunction in Alzheimer's Disease. *Cell Metab* 30 (3):493-507.e496.

Ballou, L.M., and R.Z. Lin, 2008 Rapamycin and mTOR kinase inhibitors. *J Chem Biol* 1 (1-4):27-36.

Barnham, K.J., C.L. Masters, and A.I. Bush, 2004 Neurodegenerative diseases and oxidative stress. *Nat Rev Drug Discov* 3 (3):205-214.

Bertinato, J., M. Iskandar, and M.R. L'Abbé, 2003 Copper deficiency induces the upregulation of the copper chaperone for Cu/Zn superoxide dismutase in weanling male rats. *J Nutr* 133 (1):28-31.

Blackman, R.K., K. Cheung-Ong, M. Gebbia, D.A. Proia, S. He *et al.*, 2012 Mitochondrial electron transport is the cellular target of the oncology drug elesclomol. *PLoS One* 7 (1):e29798.

Bodineau, C., M. Tomé, P.D.S. Murdoch, and R.V. Durán, 2022 Glutamine, MTOR and autophagy: a multiconnection relationship. *Autophagy* 18 (11):2749-2750.

Bülow, P., A. Patgiri, and V. Faundez, 2022 Mitochondrial protein synthesis and the bioenergetic cost of neurodevelopment. *iScience* 25 (9):104920.

Camandola, S., and M.P. Mattson, 2017 Brain metabolism in health, aging, and neurodegeneration. *Embo j* 36 (11):1474-1492.

Casimir, P., R. Iwata, and P. Vanderhaeghen, 2024 Linking mitochondria metabolism, developmental timing, and human brain evolution. *Curr Opin Genet Dev* 86:102182.

Cheng, S.W., L.G. Fryer, D. Carling, and P.R. Shepherd, 2004 Thr2446 is a novel mammalian target of rapamycin (mTOR) phosphorylation site regulated by nutrient status. *J Biol Chem* 279 (16):15719-15722.

Chiang, G.G., and R.T. Abraham, 2005 Phosphorylation of mammalian target of rapamycin (mTOR) at Ser-2448 is mediated by p70S6 kinase. *J Biol Chem* 280 (27):25485-25490.

Comstra, H.S., J. McArthy, S. Rudin-Rush, C. Hartwig, A. Gokhale *et al.*, 2017 The interactome of the copper transporter ATP7A belongs to a network of neurodevelopmental and neurodegeneration factors. *Elife* 6.

Davies, K.M., S. Bohic, A. Carmona, R. Ortega, V. Cottam *et al.*, 2014 Copper pathology in vulnerable brain regions in Parkinson's disease. *Neurobiol Aging* 35 (4):858-866.

Dennis, P.B., A. Jaeschke, M. Saitoh, B. Fowler, S.C. Kozma *et al.*, 2001 Mammalian TOR: a homeostatic ATP sensor. *Science* 294 (5544):1102-1105.

Donsante, A., L. Yi, P.M. Zerfas, L.R. Brinster, P. Sullivan *et al.*, 2011 ATP7A gene addition to the choroid plexus results in long-term rescue of the lethal copper transport defect in a Menkes disease mouse model. *Mol Ther* 19 (12):2114-2123.

Faundez, V., M. Wynne, A. Crocker, and D. Tarquinio, 2019 Molecular Systems Biology of Neurodevelopmental Disorders, Rett Syndrome as an Archetype. *Front Integr Neurosci* 13:30.

Gao, W., Z. Huang, J. Duan, E.C. Nice, J. Lin *et al.*, 2021 Elesclomol induces copper-dependent ferroptosis in colorectal cancer cells via degradation of ATP7A. *Mol Oncol* 15 (12):3527-3544.

Garza, N.M., A.B. Swaminathan, K.P. Maremanda, M. Zulkifli, and V.M. Gohil, 2023 Mitochondrial copper in human genetic disorders. *Trends Endocrinol Metab* 34 (1):21-33.

Garza, N.M., M. Zulkifli, and V.M. Gohil, 2022 Elesclomol elevates cellular and mitochondrial iron levels by delivering copper to the iron import machinery. *J Biol Chem* 298 (7):102139.

Gohil, V.M., 2021 Repurposing elesclomol, an investigational drug for the treatment of copper metabolism disorders. *Expert Opin Investig Drugs* 30 (1):1-4.

Goyal, M.S., M. Hawrylycz, J.A. Miller, A.Z. Snyder, and M.E. Raichle, 2014 Aerobic glycolysis in the human brain is associated with development and neotenous gene expression. *Cell Metab* 19 (1):49-57.

Guthrie, L.M., S. Soma, S. Yuan, A. Silva, M. Zulkifli *et al.*, 2020 Elesclomol alleviates Menkes pathology and mortality by escorting Cu to cuproenzymes in mice. *Science* 368 (6491):620-625.

Haberkiewicz, O., P. Lipiński, R.R. Starzyński, A. Jończy, P. Kurowska *et al.*, 2022 Decreased Expression of the Slc31a1 Gene and Cytoplasmic Relocalization of Membrane CTR1 Protein in Renal Epithelial Cells: A Potent Protective Mechanism against Copper Nephrotoxicity in a Mouse Model of Menkes Disease. *Int J Mol Sci* 23 (19).

Heuberger, D.M., S. Harankhedkar, T. Morgan, P. Wolint, M. Calcagni *et al.*, 2019 High-affinity Cu(I) chelator PSP-2 as potential anti-angiogenic agent. *Scientific Reports* 9 (1):14055.

Huang, R., I. Grishagin, Y. Wang, T. Zhao, J. Greene *et al.*, 2019 The NCATS BioPlanet - An Integrated Platform for Exploring the Universe of Cellular Signaling Pathways for Toxicology, Systems Biology, and Chemical Genomics. *Front Pharmacol* 10:445.

Ianevski, A., A.K. Giri, and T. Aittokallio, 2020 SynergyFinder 2.0: visual analytics of multi-drug combination synergies. *Nucleic Acids Res* 48 (W1):W488-w493.

Iverson, T.M., P.K. Singh, and G. Cecchini, 2023 An evolving view of complex II-noncanonical complexes, megacomplexes, respiration, signaling, and beyond. *J Biol Chem* 299 (6):104761.

Iwata, R., P. Casimir, E. Erkol, L. Boubakar, M. Planque *et al.*, 2023 Mitochondria metabolism sets the species-specific tempo of neuronal development. *Science* 379 (6632):eabn4705.

Iwata, R., and P. Vanderhaeghen, 2024 Metabolic mechanisms of species-specific developmental tempo. *Dev Cell* 59 (13):1628-1639.

Jimenez-Blasco, D., J. Agulla, R. Lapresa, M. Garcia-Macia, V. Bobo-Jimenez *et al.*, 2024 Weak neuronal glycolysis sustains cognition and organismal fitness. *Nat Metab* 6 (7):1253-1267.

Johnson, E.C.B., E.B. Dammer, D.M. Duong, L. Ping, M. Zhou *et al.*, 2020 Large-scale proteomic analysis of Alzheimer's disease brain and cerebrospinal fluid reveals early changes in energy metabolism associated with microglia and astrocyte activation. *Nat Med* 26 (5):769-780.

Johnson, S.C., M.E. Yanos, E.B. Kayser, A. Quintana, M. Sangesland *et al.*, 2013 mTOR inhibition alleviates mitochondrial disease in a mouse model of Leigh syndrome. *Science* 342 (6165):1524-1528.

Kahlson, M.A., and S.J. Dixon, 2022 Copper-induced cell death. *Science* 375 (6586):1231-1232.

Kaler, S.G., 2011 ATP7A-related copper transport diseases-emerging concepts and future trends. *Nat Rev Neurol* 7 (1):15-29.

Khan, N.A., J. Nikkanen, S. Yatsuga, C. Jackson, L. Wang *et al.*, 2017 mTORC1 Regulates Mitochondrial Integrated Stress Response and Mitochondrial Myopathy Progression. *Cell Metab* 26 (2):419-428.e415.

Kim, B.E., M.L. Turski, Y. Nose, M. Casad, H.A. Rockman *et al.*, 2010 Cardiac copper deficiency activates a systemic signaling mechanism that communicates with the copper acquisition and storage organs. *Cell Metab* 11 (5):353-363.

Kirshner, J.R., S. He, V. Balasubramanyam, J. Kepros, C.Y. Yang *et al.*, 2008 Elesclomol induces cancer cell apoptosis through oxidative stress. *Mol Cancer Ther* 7 (8):2319-2327.

Kodama, H., and Y. Murata, 1999 Molecular genetics and pathophysiology of Menkes disease. *Pediatr Int* 41 (4):430-435.

Kunz, W.S., A.V. Kuznetsov, J.F. Clark, I. Tracey, and C.E. Elger, 1999 Metabolic consequences of the cytochrome c oxidase deficiency in brain of copper-deficient Mo(vbr) mice. *J Neurochem* 72 (4):1580-1585.

Kuzawa, C.W., H.T. Chugani, L.I. Grossman, L. Lipovich, O. Muzik *et al.*, 2014 Metabolic costs and evolutionary implications of human brain development. *Proc Natl Acad Sci U S A* 111 (36):13010-13015.

Kuznetsov, A.V., J.F. Clark, K. Winkler, and W.S. Kunz, 1996 Increase of flux control of cytochrome c oxidase in copper-deficient mottled brindled mice. *J Biol Chem* 271 (1):283-288.

La Fontaine, S., and J.F. Mercer, 2007 Trafficking of the copper-ATPases, ATP7A and ATP7B: role in copper homeostasis. *Arch Biochem Biophys* 463 (2):149-167.

Lane, A., A. Gokhale, E. Werner, A. Roberts, A. Freeman *et al.*, 2022 Sulfur- and phosphorus-standardized metal quantification of biological specimens using inductively coupled plasma mass spectrometry. *STAR Protoc* 3 (2):101334.

Lane, A.R., N.E. Scher, S. Bhattacharjee, S.A. Zlatic, A.M. Roberts *et al.*, 2025 Adaptive protein synthesis in genetic models of copper deficiency and childhood neurodegeneration. *Mol Biol Cell* 36 (3):ar33.

Lenartowicz, M., W. Krzeptowski, P. Lipiński, P. Grzmil, R. Starzyński *et al.*, 2015 Mottled Mice and Non-Mammalian Models of Menkes Disease. *Front Mol Neurosci* 8:72.

Lin, M.T., and M.F. Beal, 2006 Mitochondrial dysfunction and oxidative stress in neurodegenerative diseases. *Nature* 443 (7113):787-795.

Liu, G.Y., and D.M. Sabatini, 2020 mTOR at the nexus of nutrition, growth, ageing and disease. *Nat Rev Mol Cell Biol* 21 (4):183-203.

Liu, Q., C. Xu, S. Kirubakaran, X. Zhang, W. Hur *et al.*, 2013 Characterization of Torin2, an ATP-competitive inhibitor of mTOR, ATM, and ATR. *Cancer Res* 73 (8):2574-2586.

Lutsenko, S., 2020 Sending copper where it is needed most. *Science* 368 (6491):584-585.

Ma, X.M., and J. Blenis, 2009 Molecular mechanisms of mTOR-mediated translational control. *Nat Rev Mol Cell Biol* 10 (5):307-318.

Marroquin, L.D., J. Hynes, J.A. Dykens, J.D. Jamieson, and Y. Will, 2007 Circumventing the Crabtree Effect: Replacing Media Glucose with Galactose Increases Susceptibility of HepG2 Cells to Mitochondrial Toxicants. *Toxicological Sciences* 97 (2):539-547.

Maung, M.T., A. Carlson, M. Olea-Flores, L. Elkhadragy, K.M. Schachtschneider *et al.*, 2021 The molecular and cellular basis of copper dysregulation and its relationship with human pathologies. *Faseb j* 35 (9):e21810.

Menkes, J.H., M. Alter, G.K. Steigleder, D.R. Weakley, and J.H. Sung, 1962 A sex-linked recessive disorder with retardation of growth, peculiar hair, and focal cerebral and cerebellar degeneration. *Pediatrics* 29:764-779.

Nagai, M., N.H. Vo, L. Shin Ogawa, D. Chimmanamada, T. Inoue *et al.*, 2012 The oncology drug elesclomol selectively transports copper to the mitochondria to induce oxidative stress in cancer cells. *Free Radic Biol Med* 52 (10):2142-2150.

Natera-de Benito, D., A. Sola, P.R. Sousa, S. Boronat, J. Expósito-Escudero *et al.*, 2021 Copper Toxicity Associated With an ATP7A-Related Complex Phenotype. *Pediatr Neurol* 119:40-44.

Navé, B.T., M. Ouwens, D.J. Withers, D.R. Alessi, and P.R. Shepherd, 1999 Mammalian target of rapamycin is a direct target for protein kinase B: identification of a convergence point for opposing effects of insulin and amino-acid deficiency on protein translation. *Biochem J* 344 Pt 2 (Pt 2):427-431.

Nose, Y., B.E. Kim, and D.J. Thiele, 2006 Ctr1 drives intestinal copper absorption and is essential for growth, iron metabolism, and neonatal cardiac function. *Cell Metab* 4 (3):235-244.

Ogawa, E., and H. Kodama, 2012 Effects of disulfiram treatment in patients with Menkes disease and occipital horn syndrome. *J Trace Elem Med Biol* 26 (2-3):102-104.

Panwar, V., A. Singh, M. Bhatt, R.K. Tonk, S. Azizov *et al.*, 2023 Multifaceted role of mTOR (mammalian target of rapamycin) signaling pathway in human health and disease. *Signal Transduction and Targeted Therapy* 8 (1):375.

Perez-Gomez, R., V. Magnin, Z. Mihajlovic, V. Slaninova, and A. Krejci, 2020 Downregulation of respiratory complex I mediates major signalling changes triggered by TOR activation. *Sci Rep* 10 (1):4401.

Peterson, T.R., M. Laplante, C.C. Thoreen, Y. Sancak, S.A. Kang *et al.*, 2009 DEPTOR is an mTOR inhibitor frequently overexpressed in multiple myeloma cells and required for their survival. *Cell* 137 (5):873-886.

Pramatarova, A., D.A. Figlewicz, A. Krizus, F.Y. Han, I. Ceballos-Picot *et al.*, 1995 Identification of new mutations in the Cu/Zn superoxide dismutase gene of patients with familial amyotrophic lateral sclerosis. *Am J Hum Genet* 56 (3):592-596.

Rajan, A., and R.M. Fame, 2024 Brain development and bioenergetic changes. *Neurobiol Dis* 199:106550.

Rembach, A., D.J. Hare, M. Lind, C.J. Fowler, R.A. Cherny *et al.*, 2013 Decreased copper in Alzheimer's disease brain is predominantly in the soluble extractable fraction. *Int J Alzheimers Dis* 2013:623241.

Reynolds, T.H.t., S.C. Bodine, and J.C. Lawrence, Jr., 2002 Control of Ser2448 phosphorylation in the mammalian target of rapamycin by insulin and skeletal muscle load. *J Biol Chem* 277 (20):17657-17662.

Roberts, B.R., T.M. Ryan, A.I. Bush, C.L. Masters, and J.A. Duce, 2012 The role of metallobiology and amyloid-β peptides in Alzheimer's disease. *J Neurochem* 120 Suppl 1:149-166.

Rosen, D.R., T. Siddique, D. Patterson, D.A. Figlewicz, P. Sapp *et al.*, 1993 Mutations in Cu/Zn superoxide dismutase gene are associated with familial amyotrophic lateral sclerosis. *Nature* 362 (6415):59-62.

Sakai, D., Y. Murakami, D. Shigeta, M. Tomosugi, H. Sakata-Haga *et al.*, 2023 Glycolytic activity is required for the onset of neural plate folding during neural tube closure in mouse embryos. *Front Cell Dev Biol* 11:1212375.

Scheiber, I.F., J.F. Mercer, and R. Dringen, 2014 Metabolism and functions of copper in brain. *Prog Neurobiol* 116:33-57.

Schrag, M., C. Mueller, U. Oyoyo, M.A. Smith, and W.M. Kirsch, 2011 Iron, zinc and copper in the Alzheimer's disease brain: a quantitative meta-analysis. Some insight on the influence of citation bias on scientific opinion. *Prog Neurobiol* 94 (3):296-306.

Soma, S., A.J. Latimer, H. Chun, A.C. Vicary, S.A. Timbalia *et al.*, 2018 Elesclomol restores mitochondrial function in genetic models of copper deficiency. *Proc Natl Acad Sci U S A* 115 (32):8161-8166.

Steiner, P., 2019 Brain Fuel Utilization in the Developing Brain. *Ann Nutr Metab* 75 Suppl 1:8-18.

Terada, T., T. Obi, T. Bunai, T. Matsudaira, E. Yoshikawa *et al.*, 2020 In vivo mitochondrial and glycolytic impairments in patients with Alzheimer disease. *Neurology* 94 (15):e1592-e1604.

Tokuda, E., and Y. Furukawa, 2016 Copper Homeostasis as a Therapeutic Target in Amyotrophic Lateral Sclerosis with SOD1 Mutations. *Int J Mol Sci* 17 (5).

Tracey, I., J.F. Dunn, and G.K. Radda, 1997 A 31P-magnetic resonance spectroscopy and biochemical study of the mo(vbr) mouse: potential model for the mitochondrial encephalomyopathies. *Muscle Nerve* 20 (11):1352-1359.

Tsang, T., C.I. Davis, and D.C. Brady, 2021 Copper biology. *Curr Biol* 31 (9):R421-r427.

Tsang, T., J.M. Posimo, A.A. Gudiel, M. Cicchini, D.M. Feldser *et al.*, 2020 Copper is an essential regulator of the autophagic kinases ULK1/2 to drive lung adenocarcinoma. *Nat Cell Biol* 22 (4):412-424.

Tsvetkov, P., S. Coy, B. Petrova, M. Dreishpoon, A. Verma *et al.*, 2022 Copper induces cell death by targeting lipoylated TCA cycle proteins. *Science* 375 (6586):1254-1261.

Tümer, Z., and L.B. Møller, 2010 Menkes disease. *Eur J Hum Genet* 18 (5):511-518.

Vest, K.E., A.L. Paskavitz, J.B. Lee, and T. Padilla-Benavides, 2018 Dynamic changes in copper homeostasis and post-transcriptional regulation of Atp7a during myogenic differentiation. *Metallomics* 10 (2):309-322.

Wallace, D.C., 2005 A mitochondrial paradigm of metabolic and degenerative diseases, aging, and cancer: a dawn for evolutionary medicine. *Annu Rev Genet* 39:359-407.

Wang, Y., and S. Hekimi, 2021 Minimal mitochondrial respiration is required to prevent cell death by inhibition of mTOR signaling in CoQ-deficient cells. *Cell Death Discovery* 7 (1):201.

Wilschefski, S.C., and M.R. Baxter, 2019 Inductively Coupled Plasma Mass Spectrometry: Introduction to Analytical Aspects. *Clin Biochem Rev* 40 (3):115-133.

Wu, L., L. Zhou, D.Q. Liu, F.G. Vogt, and A.S. Kord, 2011 LC-MS/MS and density functional theory study of copper(II) and nickel(II) chelating complexes of elesclomol (a novel anticancer agent). *J Pharm Biomed Anal* 54 (2):331-336.

Yadav, B., K. Wennerberg, T. Aittokallio, and J. Tang, 2015 Searching for Drug Synergy in Complex Dose-Response Landscapes Using an Interaction Potency Model. *Comput Struct Biotechnol J* 13:504-513.

Yuan, S., T. Korolnek, and B.E. Kim, 2022 Oral Elesclomol Treatment Alleviates Copper Deficiency in Animal Models. *Front Cell Dev Biol* 10:856300.

Zeng, H., J.T. Saari, and W.T. Johnson, 2007 Copper deficiency decreases complex IV but not complex I, II, III, or V in the mitochondrial respiratory chain in rat heart. *J Nutr* 137 (1):14-18.

Zheng, X., L. Boyer, M. Jin, J. Mertens, Y. Kim *et al.*, 2016 Metabolic reprogramming during neuronal differentiation from aerobic glycolysis to neuronal oxidative phosphorylation. *Elife* 5.

Zheng, X., S. Narayanan, C. Xu, S. Eliasson Angelstig, J. Grünler *et al.*, 2022 Repression of hypoxia-inducible factor-1 contributes to increased mitochondrial reactive oxygen species production in diabetes. *Elife* 11.

Zheng, Y., and Y. Jiang, 2015 mTOR Inhibitors at a Glance. *Mol Cell Pharmacol* 7 (2):15-20.

Zlatic, S., H.S. Comstra, A. Gokhale, M.J. Petris, and V. Faundez, 2015 Molecular basis of neurodegeneration and neurodevelopmental defects in Menkes disease. *Neurobiol Dis* 81:154-161.

Zlatic, S.A., A. Vrailas-Mortimer, A. Gokhale, L.J. Carey, E. Scott *et al.*, 2018 Rare Disease Mechanisms Identified by Genealogical Proteomics of Copper Homeostasis Mutant Pedigrees. *Cell Syst* 6 (3):368-380.e366.

Supplemental Information

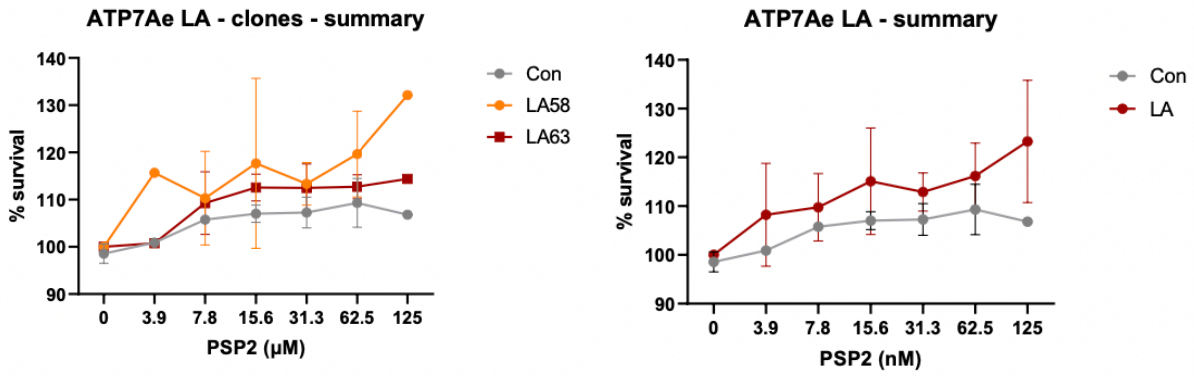

Supplemental Figure 1. Percent survival of ATP7A control vs. ATP7A mutant cells across increasing concentrations of PSP2 (n=2 for controls and mutants), representing percent survival relative to untreated cells. There is a difference in the response to varying concentrations of the drug, with possible increase of survival in our LA mutants compared to the controls from use of an undetermined pathway.

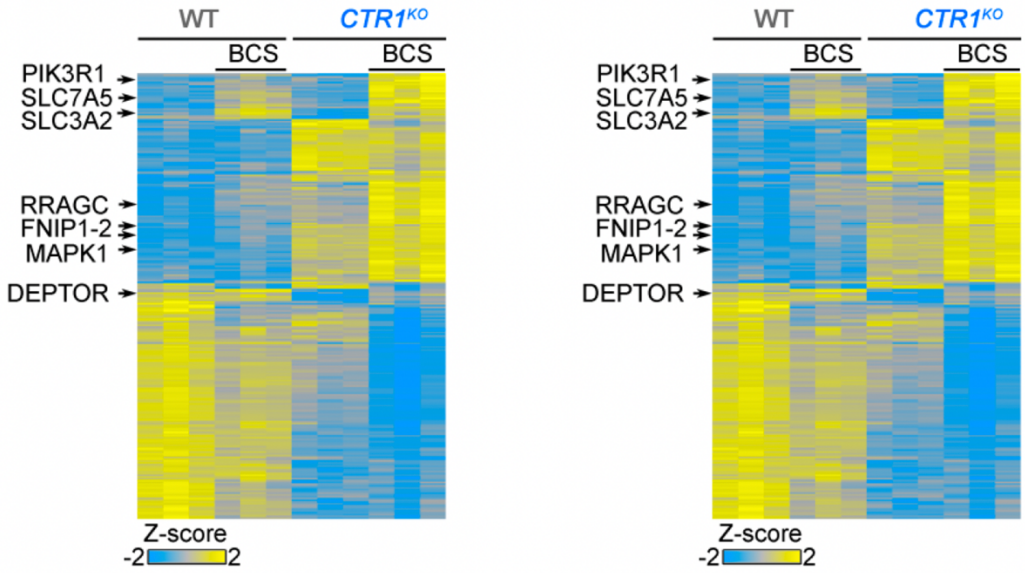

Supplemental Figure 2. Hierarchial clustering of the metabolism annotated transcriptome differentially expressed at a significancy of q<0.05 (analyzed by a one-way ANOVA followed by Benjamini-Hochberg FDR correction).